Curve number for runoff estimating in interlocking concrete pavement

Curva número para estimativa do escoamento superficial em pavimento de concreto intertravado

Murilo Cesar Lucas[1] , Gustavo Bonfim Jodas[1] , Luis Eduardo Bertotto[2] ,
Paulo Tarso Sanches de Oliveira[3] , Alessandro Bail[4]

[1]Universidade Tecnológica Federal do Paraná, Pato Branco, PR, Brasil
[2]Universidade de São Paulo, São Carlos, SP, Brasil
[3]Universidade Federal do Mato Grosso do Sul, Mato Grosso do Sul, MS, Brasil
[4]Universidade Tecnológica Federal do Paraná, Londrina, PR, Brasil
E-mails: muriloclucas@gmail.com, (MCL), gustavojodas@alunos.utfpr.edu.br, (GBJ), bertotto@usp.br, (LEB),
paulotarsoms@gmail.com (PTSO), alebail@utfpr.edu.br (AB)

ABSTRACT

Curve Number (CN) values estimating from rainfall-runoff data is an attractive topic in hydrology. However, CN values are lacking for Interlocking Concrete Pavement (ICP) material, mainly when seated over bare soil (not over a permeable pavement structure). Here, we compute CN values for the ICP seated over clayey soil using measured rainfall and infiltration capacity data. We estimated runoff (Q) using 32 events of 24-hour rainfall depth (P_{24}) and an infiltration model, assuming a hortonian runoff process. To estimate the CN for each P_{24} event, we used the rainfall-runoff incremental approach. Overall, we obtained CN values ranging from 52 to 63. The best CN values to estimate Q were equal to 52.2 ($RMSE = 9.09$ mm and $R^2 = 0.03$) and 60.1 ($RMSE = 1.45$ mm and $R^2 = 0.97$), considering natural- and rank-ordered P_{24}-Q data, respectively. Our results indicate that it is more suitable to use the initial abstraction ratio (λ) equal to 0.20 for the ICP material. The findings provide a better understanding of the rainfall-runoff process in ICP and help improve the design of stormwater drainage systems.

Keywords: Paver; Low impact development systems; Stormwater Drainage System; Flooding.

RESUMO

A estimativa de valores Curva Número (CN) a partir de dados chuva-vazão é um tópico atrativo em hidrologia. No entanto, há carência de valores de CN para o material Pavimento de Concreto Intertravado (PCI), particularmente quando assentado sobre o solo exposto (não sobre uma estrutura de pavimentos permeáveis). Aqui, nós calculamos valores de CN para o PCI assentado sobre solo argiloso e usando dados medidos de chuva e capacidade de infiltração. Nós estimamos o escoamento superficial (Q) usando dados de altura de chuva com duração de 24 horas (P_{24}) junto com um modelo de infiltração, sob a hipótese do processo hortoniano de geração de Q. Para estimar o valor de CN para cada evento de chuva, nós adotamos a abordagem incremental do tipo chuva-vazão. Nós obtivemos valores de CN variando de 52 ($RMSE = 9,09$ mm and $R^2 = 0,03$) a 63 ($RMSE = 1,45$ mm and $R^2 = 0,97$). Resumidamente, os melhores valores de CN foram iguais a 52,2 e 60,1, considerando os dados P_{24}-Q ordenados naturalmente e ranqueados, respectivamente. Nossos resultados indicam que é melhor usar um valor de taxa de abstração inicial (λ) igual a 0,20 para o material PCI. As descobertas fornecem um melhor entendimento sobre o processo chuva-vazão no material PCI e ajudam a aprimorar projetos de sistemas de drenagem pluvial.

Palavras-chave: Paver; Sistemas de baixo Impacto de Desenvolvimento; Sistemas de drenagem pluvial; Inundações.

INTRODUCTION

Water resources engineers face the challenge of estimating stormwater runoff, primarily for applications in flood control design and early flood warning systems in urban areas and soil and water conservation practices in agricultural/natural land. Traditionally, engineers have dealt with the aforementioned applications in small and ungauged watersheds by transforming rainfall depth into runoff depth (Grimaldi et al., 2013) using a rainfall-runoff model.

In the mid-1950s, the Soil Conservation Service's Curve Number method (CN method) arose as a mathematically simple, low-cost, and versatile rainfall-runoff model. This method is catchy because only rainfall depth (variable input) and CN (parameter) are required to estimate runoff. Further, it is versatile because CN values are tabulated in the National Engineering Handbook, Section 4 (NEH4), of the US Department of Agriculture (United States Department of Agriculture, 2004), for several land use and cover and soil types (Hydrologic Soil Groups, HSG).

The CN method was solely developed to assess the influence of land use and cover modification in runoff for small agricultural watersheds (Ponce & Hawkins, 1996). Over time, practical engineers have extended the application of the CN method for designing stormwater drainage systems in urban watersheds (United States Department of Agriculture, 1986). The CN method is also applied in incremental rainfall amounts with an associated watershed unit-hydrograph to estimate runoff hydrographs (Chin, 2021). The CN method was not originally intended to be used in incremental rainfall amounts less than the duration of the 24-hour rainfall (Karpathy & Chin, 2019). Here, we referred to this as the INCremental RAinfall-RUNoff (INCRARUN) approach.

The CN method's limitations are widely reported (Ajmal et al., 2016; Chin, 2021; Hawkins, 1993, 2014; Jain et al., 2006; Michel et al., 2005; Ponce & Hawkins, 1996; Sahu et al., 2012; Shi et al., 2021; Verma et al., 2020). Nevertheless, researchers still make efforts to soften these limitations by adjusting the CN method's formulation or estimating CN values for specific site features. Applying the INCRARUN approach using the CN tabulated values invokes at least two limitations (Chin, 2021). First is the lack of consideration of variation in rainfall characteristics. Second, it does not constrain the infiltration rate to be less than or equal to the infiltration capacity of the watershed. To overcome these limitations, a few studies have combined an infiltration model with 24-hour hyetographs to estimate the CN parameter (e.g., Bertotto et al., 2021; Chin, 2017).

Studies have focused on CN estimating for crops (Durán-Barroso et al., 2017; Lal et al., 2017), undisturbed vegetation (Oliveira et al., 2016), and forests (Im et al., 2020). However, CN values are lacking for Interlocking Concrete Pavement (ICP) material. This is an imporante issue because ICP is commonly used as a wear layer of permeable pavements (i.e., Permeable Interlocking Concrete Paver, PICP) (Beecham et al., 2012; Lucke et al., 2015) in sidewalks and parking lots. PICP is recognized as a SUstainable Drainage System (SUDS) because it can mitigate urban flooding significantly by reducing runoff peak and volumes (Collins et al., 2008; Liu et al., 2020; Palla & Gnecco, 2015; Winston et al., 2019) and pollutant loading (Legret et al., 1999; Pratt et al., 1999), mimicking the pre-development hydrologic conditions (Woods-Ballard et al., 2015).

To our knowledge, few studies have reported the CN values for the PICP using measured rainfall and runoff data (e.g., Bean et al., 2007). Schwartz (2010) adopted design rainfall and infiltration capacity of the subgrade soil to simulate runoff and the CN for permeable pavements. Martin & Kaye (2014) used design rainfall and the theoretical framework from Schwartz (2010) to present a generalized method for calculating the CN for permeable pavements. Damodaram et al. (2010) validated a CN estimating approach for permeable pavements using three rainfall-runoff datasets of the literature.

In Brazil, the decision-makers have commonly employed the ICP material over bare soil (not over a permeable pavement structure) to save financial costs. However, CN estimates from field data for this situation are even scarce. To fill this gap, we focus on estimating the CN parameter for interlocking concrete pavement seated over low-permeability clayey soil. We investigated the ICP surface under clogging and unclogging conditions. Our CN values account for intrarainfall variability and infiltration capacity data in the study area.

MATERIALS AND METHODS

Study area

This study was developed at the Federal University of Technology - Parana (UTFPR) in the municipality of Pato Branco, located southwest of Parana State, southern Brazil (26°19' S, 52°69' W) (Figure 1).

The Pato Branco city Hall has decreed the mandatory use of ICP in the sidewalks (3037 Law) since 2008, leading to extensive adoption of this material as a wear layer, mainly the downtown. This municipality Law aims to increase infiltration and reduce runoff in the urban area.

According to Köppen's climate classification, the climate in the study area is the temperate oceanic climate (Cfb), humid subtropical with temperate summer and without a dry season

Geographic Information Systems, datum: SIRGAS 2000.
Cartographic base: IBGE (2021).
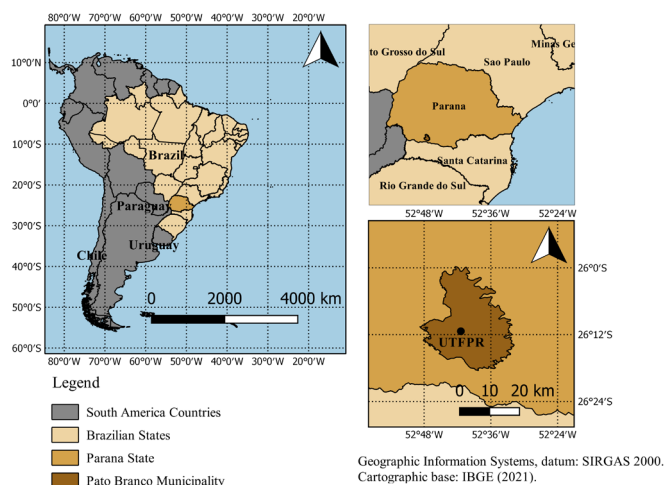
Figure 1. Location of the study area. The eight infiltration tests were performed at the Federal University of Technology - Parana (UTFPR) in the municipality of Pato Branco.

(Alvares et al., 2013). The annual average precipitation ± standard deviation is 1994 ± 487.8 mm between 1965 and 2021. Tabalipa (2008) observed high clay (64.4%) and silt (29.3%) content in the soil samples (1.5 m of depth) around the UTFPR area. Hence, according to USDA (United States Department of Agriculture, 2004), the HSG around the UTFPR is classified as type D.

Study delineation

To estimate runoff depth for the ICP material, we used the methodology proposed by Chin (2017). The study delineation is summarized in Figure 2.

We first graphed the 32 hyetographs using 24-hour rainfall depth (P_{24}) data at 10-minutes time steps. Thus, measured rainfall was used here instead of design rainfall. Second, to adjust an infiltration curve model, we used field infiltration data of the ICP surface. Third, to estimate runoff for each P_{24} event, we combined the infiltration model and hyetographs. Then, to adjust the best CN value using the CN method's formulation, we related P_{24} and runoff (Q) datasets (P_{24}- Q).

24-hour hyetographs

The 24-hour rainfall depth (P_{24}) data came from the Center for Natural Disaster Monitoring and Alert (CEMADEN). The automatic tipping-bucket rain gauge (411850104A station) records rainfall depth every 10 minutes during the event and records

zero value (absence of rainfall) every 1 hour. The CEMADEN does not perform a consistent analysis of rainfall data before it is available at Mapa Interativo (Brasil, 2022).

We used 32 P_{24} events to generate hyetographs at sequential 10-minute time intervals (Supplementary Material Table S1). The hyetographs of P_{24} were transformed into rainfall intensity hyetographs, i. We selected P_{24} events randomly ranging from 0 to 150 mm over the 2014-2021 period. The range of rainfall depths was chosen to account for different rainfall characteristics (distribution, return period, and intensity) for the analysis of the P_{24}- Q data.

Infiltration capacity

The infiltration capacity data came from Bazzo & Horn (2017). Eight infiltration tests were conducted for ICP *in situ* using a single-ring infiltrometer at the sidewalks of the Federal University of Technology – Parana during August in 2017 year. The sidewalks are made of ICP material seated over bare soil. Bazzo & Horn (2017) performed infiltration tests under clogging and unclogging conditions on the ICP surface (four tests in each ICP condition). To perform infiltration tests, they adopted a modified version of the single-ring infiltration method for permeable pavement structures (American Society for Testing and Materials, 2013), because the ICP is seated over bare soil.

A 0.30 m-diameter infiltrometer ring was placed over the ICP surface (sidewalks). Following Bean et al. (2007), Bazzo & Horn (2017) molded a thin ribbon of plumber's putty along the
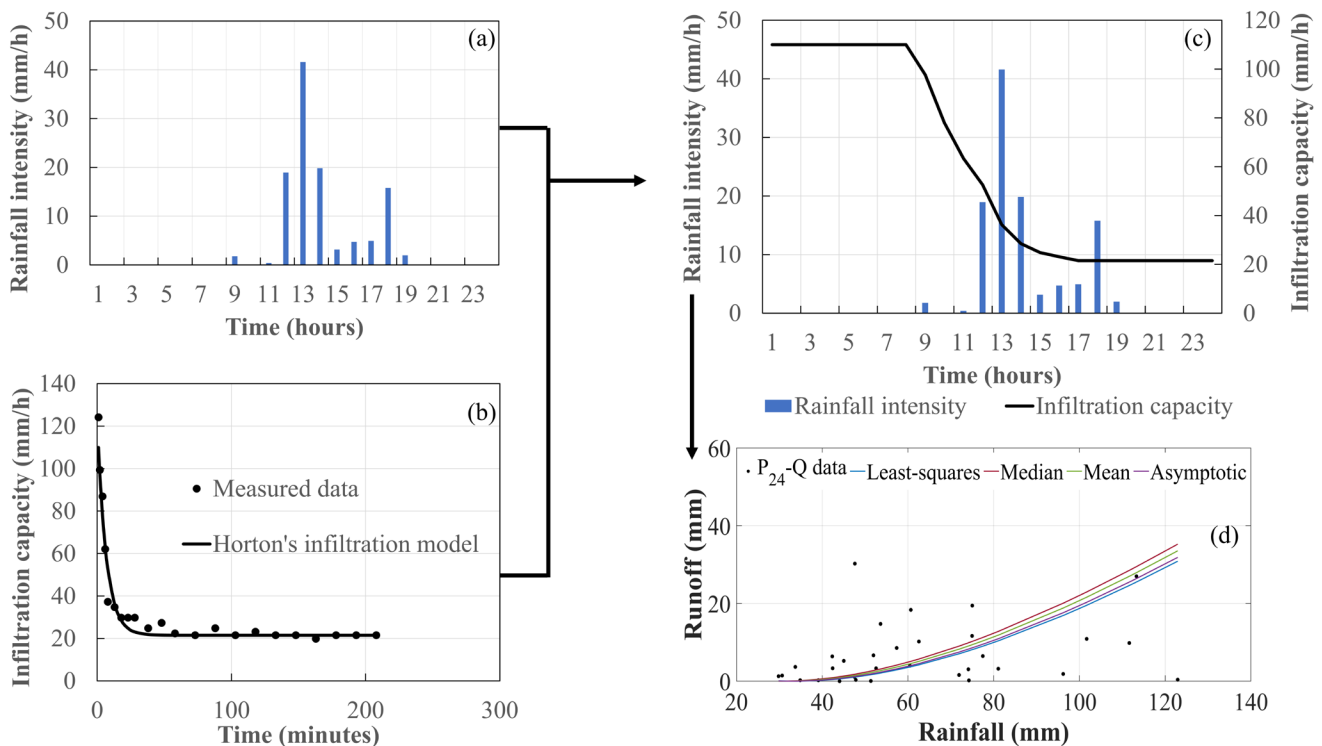
Figure 2. Study delineation for Curve Number (CN) estimating in the Interlocking Concrete Pavement (ICP). The black arrows indicate the path of the main methodological steps: (a) The 24-hour hyetograph; (b) The Horton's model fitted against infiltration capacity data; (c) The combined infiltration model and hyetograph to estimate runoff; and (d) The runoff estimation according to rainfall depth using different methods for CN adjusting (least-squares, median, mean, and asymptopic fit).

ring's bottom (Figure 3). To avoid leakage, the putty was depressed, forming a tight seal between the ICP surface and the ring.

After the ring was filled with freshwater, water level drops were measured over time (variable-head). When the water level dropped to 1/3 of its initial level, water volume was added until it rose to the initial level. The infiltration rate was calculated by dividing the flow rate by the cross-sectional area of the ring. The tests were finished three (equal) consecutive values of infiltration rate were achieved.

We fitted Horton's infiltration model (Horton, 1933) against the infiltration capacity data using the Levenberg-Marquardt method (Levenberg, 1944; Marquardt, 1963) for nonlinear least-squares problems. Because the water was ponded above the ICP surface, we assumed that the infiltration rate equals the infiltration capacity. The empirical Horton's equation can be written as:

$$f_p = f_c + (f_0 - f_c)e^{-\beta.t} \tag{1}$$

Where f_p is the infiltration capacity ($\mathrm{mm.h^{-1}}$) at time, t (h), f_0 is the initial infiltration capacity ($\mathrm{mm.h^{-1}}$), f_c is the asymptotic (steady) infiltration capacity ($\mathrm{mm.h^{-1}}$), and β is the Horton's decay parameter ($\mathrm{h^{-1}}$). We measured f_p and f_0 from infiltration tests, while β and f_c (Equation 1) were fitted using the Levenberg-Marquardt method in the MATLAB Curve Fitting Toolbox, version 2021a.

Hortonian runoff processes for runoff calculation

Background

Most studies have estimated the CN parameter using measured P_{24} and Q data at the plot scale (e.g., Cao et al., 2011; Lal et al., 2017; Liu et al., 2018; Oliveira et al., 2016) and at the watershed scale (e.g., Assaye et al., 2021; Galbetti et al., 2021). Due to the lack of measured Q data at the watershed scale, researchers have applied filtering techniques in observed streamflow data to separate baseflow and Q components for estimating CN (D'Asaro et al., 2014; Valle Junior et al., 2019).

In this paper, we used the alternative methodology presented by Chin (2017) for estimating the CN parameter. We named this combined method generically as HORTOnian RUNoff

Figure 3. Example of the 0.30 m-diameter infiltrometer ring placed over the ICP surface.

(HORTORUN) method. The method does not differ in finding the best-fitted CN that matches Q versus P_{24} relation. However, instead of using measured Q from a given P_{24} event at plot or watershed scales, the Q values were estimated by combining the INCRARUN approach with Horton's infiltration model.

In the HORTORUN approach, runoff occurs when rainfall intensity exceeds the surface infiltration capacity. Additionally, runoff can occur due to the water-table rise above the ground surface (Dingman, 2015). This saturation from the below mechanism is usually called Dunne overland flow. Two assumptions underlay the HORTORUN method: i) Hortonian runoff process is mandatory, and ii) infiltration is the dominant process during initial abstraction and runoff until the end of the rainfall event, meaning that other abstraction processes such as interception, surface storage, and evaporation are not considered (Chin, 2017).

One advantage of this method is that the CN parameter can be related to field-measurable parameters of the infiltration process (Chin, 2017), whereas measured Q data are not required. Further, the HORTORUN method does not violate hydrologic principles when applied in incremental rainfall-runoff amounts. On the other hand, the typical application of the CN method in incremental time intervals results in infiltration that exceeds the watershed's infiltration capacities (Chin, 2021). A detailed relationship between the infiltration model and the CN method is presented by Lal et al. (2017) and Karpathy & Chin (2019).

Regardless the scale analysis, studies usually related P_{24}-Q data in two ways: natural- and rank-ordered. The rationale for using rank-ordered data is that the CN method is used to predict Q values having the same exceedance probability as the corresponding P_{24} value (Chin, 2021). While, the natural-ordered data consist of the actual observed P_{24}-Q dataset. Becase there is no concensus to the usage of rank-ordered data among hydrologists (Moglen et al., 2022), we used both approaches here.

Calculation procedure

We calculated incremental runoff using Horton's infiltration model and sequential 10-minutes time intervals for each rainfall-intensity hyetograph. We implemented the HORTORUN method in the Python programming language to optimize the calculation and decrease the chance of freehand miscalculation. We organized the HORTORUN method into six procedures keeping the original ideas presented by Chin (2017) as follows:

Procedure 1 (the conversion of rainfall hyetographs units): The rainfall intensity hyetograph is calculated using a 24-hour rainfall depth hyetograph. If ΔP_j is the incremental rainfall during the jth time interval, Δt, then the average intensity during the jth time interval is calculated as $i_j = \dfrac{\Delta P_j}{\Delta t}$.

Procedure 2 (the incremental runoff calculation): Incremental runoff at the jth time interval, ΔQ_j, is determined only in the occurrence of ponding on the ground surface. In this case, a simple water balance equation is applied as $\Delta Q_j = (\Delta P_j - \Delta I_j)$, where ΔI_j is the incremental cumulative infiltration and Δ represents the difference between the initial (t) and final ($t+1$) value at the jth time interval; for instance, $\Delta I_j = (I_j^{t+1} - I_j^t)$. Contrary, if all the rainfall during the Δt infiltrates, then $\Delta Q_j = 0$.

The runoff, Q, is the sum of all incremental runoff values $(Q = \sum_{j=1}^{n} \Delta Q_j)$ for a given P_{24} event. To calculate ΔI_j, infiltration capacity is evaluated against rainfall intensity as described in Procedure 3.

Procedure 3: (the choice of infiltration equations): The infiltration capacity at the beginning of the jth time interval, $f_{p_j}^t$, is determined from the known value of I_j^t under two conditions: i) continuous ponded ground surface and ii) noncontinuous ponded ground surface from the beginning of rainfall event.

The Horton's infiltration model for f_p (Equation 1) is valid under continuous ponding conditions, and I is given by:

$$I = f_c.t + \frac{f_0 - f_c}{\beta}\left(1 - e^{-\beta.t}\right) \tag{2}$$

However, Horton's infiltration model is not valid under noncontinuous ponding condition. Hence, infiltration capacity is a function of the cumulative infiltration given by (Chin, 2013):

$$I = \left[\frac{f_c}{\beta}\ln(f_0 - f_c) + \frac{f_0}{\beta}\right] - \frac{f_c}{\beta}\ln(f_p - f_c) - \frac{f_p}{\beta} \tag{3}$$

Procedure 4 (the evaluation of infiltration condition): If $f_{p_j}^t > i_j^t$ during the jth time interval, then it is assumed that all the rainfall during the Δt infiltrates. Thus, $\Delta Q_k = 0$, and $\Delta I_k = \Delta P_k$. It must be noted that I_j^t is known, and consequently, Equation 3 can be solved as a function of $f_{p_j}^t$.

If $f_{p_j}^t \leq i_j^t$, then the rainfall infiltrates at the f_{p_j} during the Δt. In this case, if ponding is noncontinuous, the calculation of the ΔI_j is obtained based on the shifting of the noncontinuous to the continuous ponding condition. At first, if I_j^t is the cumulative infiltration under noncontinuous ponding, then the reference time, t', to infiltrate the same I_j^t under continuous ponding condition is calculated by:

$$I = f_c.t' + \frac{f_0 - f_c}{\beta}\left(1 - e^{-\beta.t'}\right) \tag{4}$$

Horton's equation for cumulative infiltration is implicit in t' (Equation 4), where t' is the unknown value. Next, the cumulative infiltration values are calculated based on the continuous ponding assumption. Thus, Equation 4 becomes Equation 5 to calculate $I_j^{t}{}^1$ and Equation 1 is used to obtain $f_{p_j}^{t+1}$.

$$I = f_c\left(t' + \Delta t\right) + \frac{f_0 - f_c}{\beta}\left(1 - e^{-\beta\left(t' + \Delta t\right)}\right) \tag{5}$$

Particularly if this is the first Δt that runoff occurs (i.e., $\Delta Q_j^t \neq 0$), then the cumulative infiltration up to the beginning of the time interval is equal to the initial abstraction, I_a, hence $I_a = I_j^t$.

Procedure 6 (the implementation in a programming language): The previous procedures are applied sequentially in each kth time interval for all the 32 rainfall events.

2.6 Curve Number estimating

The CN method is semiempirical and relates rainfall depth to the corresponding runoff depth based on the water balance equation. The CN method formulation is given by (United States Department of Agriculture, 1986):

$$Q = \frac{\left(P - I_a\right)^2}{\left(P - I_a\right) + S}, \text{ for } P > I_a; \text{ otherwise, } Q = 0 \tag{6}$$

Where P is the rainfall depth (mm), I_a is the initial abstraction before runoff begins (mm), and F is the cumulative infiltration after runoff begins (mm), S is the potential maximum watershed storage (mm).

One assumption is that I_a occurs before Q begins (Chin, 2021), and it represents a fraction of the S thought the relationship:

$$I_a = \lambda.S \tag{7}$$

Where λ is the initial abstraction coefficient (dimensionless). Currently, this parameter is set as $\lambda = 0.20$ (United States Department of Agriculture, 1986). However, an update for the use of $\lambda = 0.05$ is in progress (United States Department of Agriculture, 2017), which is supported by some studies (Durán-Barroso et al., 2017; Valle Junior et al., 2019; Woodward et al., 2003).

The potential maximum watershed storage in Equation 6 is scaled into a tabulated Curve Number, CN (dimensionless), which varies in the range $0 \leq CN \leq 100$. The transformation of S into CN results in:

$$CN = \frac{25.400}{\left(254 + S\right)} \tag{8}$$

We estimated the CN value for each of the 32 rainfall events using the presented CN method formulation. First, S was calculated for $\lambda = 0.20$ ($S_{0.20}$) as (Hawkins, 1993):

$$S_{0.20} = 5\left(\left(P + 2Q\right) - \sqrt{4Q^2 + P.Q}\right) \tag{9}$$

Then, S was calculated for $\lambda = 0.05$ ($S_{0.05}$) as (Valle Junior et al., 2019):

$$S_{0.05} = 10\left(\left(2P + 19Q\right) - \sqrt{361Q^2 + 80P.Q}\right) \tag{10}$$

Next, CN was estimated via Equation 8. Last, we assessed a representative value of the CN using the well-accepted methods: asymptotic fit (Hawkins, 1993), least-squares (Hawkins, 1993), and central tendency (arithmetic mean, $\overline{CN}$, and median, $\widetilde{CN}$). Hawkins (1993) noticed three types of behavior using the asymptotic fit method: standard, complacent, and violent. The standard behavior occurs when the CN values decline with increasing rainfall depth until reaching an asymptotic CN value, CN_∞ (dimensionless). The standard asymptotic fit method is mathematically written as (Hawkins, 1993):

$$CN\left(P_{24}\right) = CN_\infty + \left(100 - CN_\infty\right)e^{-k.P_{24}} \tag{11}$$

Where $CN\left(P_{24}\right)$ is the CN as a function of P_{24} and k is the decay coefficient (mm^{-1}). In Equation 11, both CN_∞ and k are adjusting parameters.

The complacent behavior profile is a decline in CN with increasing rainfall depth but without reaching an asymptotic value.

If complacent behavior is presented, the CN method is unsuitable for the study area (Hawkins, 1993). The violent behavior depicted a decline in CN values until a threshold rainfall depth (P_s) and then increases suddenly with increasing rainfall depth (Hawkins, 1993). The violent behavior is expressed as (D'Asaro et al., 2014):

$$\text{CN}(P_{24}) = \text{CN}_\infty \left(1 - e^{-k_v \cdot (P_{24} - P_s)} \right) \tag{12}$$

Where k_v is a coefficient (mm^{-1}), and both CN_∞ and k_v are adjusting parameters.

We performed the asymptotic fit method using the MATLAB Curve Fitting Toolbox, version 2021a. In addition, we also solved the least-squares method using MATLAB nonlinear least-squares algorithm. The performance of the CN estimating methods was evaluated by employing metrics of error and agreement. We chose the Root Mean Square Error (*RMSE*) and determination coefficient (R^2) to quantify the average error and the goodness-of-fit, respectively.

RESULTS AND DISCUSSION

Infiltration curves and runoff calculation

Results show that f_0 and f_c ranged from 258.00 to 96.00 mm.h^{-1} and from 46.80 to 19.20 mm.h^{-1}, respectively, for clogged ICP (Figure 4). The Horton's decay parameter varied from 13.05 to 3.17 h^{-1}. (Figure 4). While for unclogged ICP, f_0

and f_c varied between 927.60 and 68.40 mm.h^{-1} and between 104.40 and 27.00 mm.h^{-1}, respectively, and β varied from 7.32 to 2.38 h^{-1}. Thus, we found that, on average, clogged ICP showed lower values of f_0 and f_c than unclogged ICP. This is expected because clogged ICP has solid sediments (dust, mosses, and twigs) between the joints that decreases infiltration capacity. The results of f_0 for clogged ICP are, on average, closed to those reported for dry clayey soil (173.83 mm.h^{-1}) by Bertotto et al. (2021) in the Pato Branco city. On the other hand, the results of f_c for clogged ICP are much higher than those for clayey soil (9.93 mm.h^{-1}) (i.e., Bertotto et al., 2021).

We assessed the descriptive statistics of f_0, f_c, and β for clogged and unclogged ICP. Because there were no outliers, we used the arithmetic mean of f_0, f_c, and β to generate a single representative Horton's model for each ICP surface condition. Hence, we calculated an average value of $f_0 = 157.50$ mm.h^{-1}, $f_c = 29.25$ mm.h^{-1}, and $\beta = 7.38$ h^{-1} for the ICP clogging condition, while for unclogged ICP, the average values were $f_0 = 429.00$ mm.h^{-1}, $f_c = 64.20$ mm.h^{-1}, and $\beta = 4.96$ h^{-1}. These average values were used to calculate the runoff through the HORTORUN approach.

We presented the runoff and CN results solely for the ICP clogging condition because runoff was not generated ($Q = 0$ mm) under the unclogged ICP. Results showed poor agreement and high scattered ($r = 0.30$) for natural-ordered P_{24}-Q data (Figure 5a), whereas rank-ordered P_{24}-Q data showed very good agreement and low scattered ($r = 0.93$) (Figure 5b).

The poor agreement in natural-ordered data means that runoff depth did not increase as rainfall depth increased because similar P_{24} events generated very different Q values (Figure 5a).
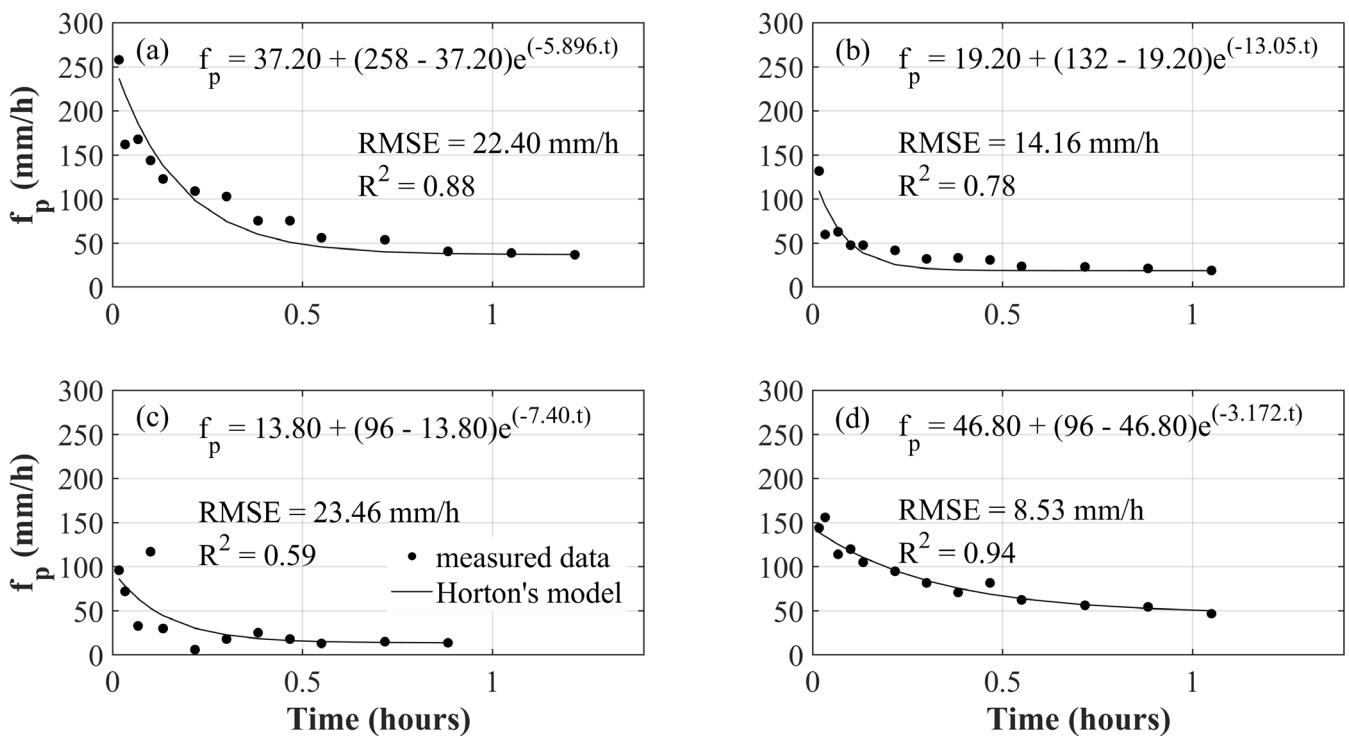
Figure 4. The fit between measured infiltration capacity and Horton's model. Four infiltration tests (a); (b); (c); and (d) were performed for the ICP clogging condition. *RMSE* is the Root Mean Squared Error, R^2 is the coefficient of determination, f_p is the infiltration capacity during the time, t.

For instance, two similar P_{24} events of 111.6 and 113.5 mm generated Q values of 9.8 and 26.9 mm, respectively (Figure 5a). Further, we noted that the largest P_{24} event (122.9 mm) lead to small Q value (0.40 mm), whereas the smallest P_{24} event (47.6 mm) generated the largest Q value (30.2 mm) (Figure 5a). This occurs because the event of $P_{24} = 113.5$ mm is less uniformly distributed and presents greater rainfall intensities exceeding infiltration capacities (Figure 6a) than the event of $P_{24} = 111.6$ (Figure 6b), both within the 24-hour standardized duration.

Similarly, it is apparent that the event of $P_{24} = 47.6$ mm is shortly distributed and has high intensity (Figure 6c), while the event of $P_{24} = 122.9$ has long distribution and low intensity (Figure 6d). Thus, our results indicate that rainfall temporal distribution within the standard duration (24-hour) strongly affects runoff generation and, ultimately, the CN estimating. Hu et al. (2020) obtained similar results at the watershed scale and found that accounting for rainfall intensity in the CN method improved runoff calculations. Chin (2021) demonstrated that rainfall distribution is essential in determining the appropriate CN value across the United States
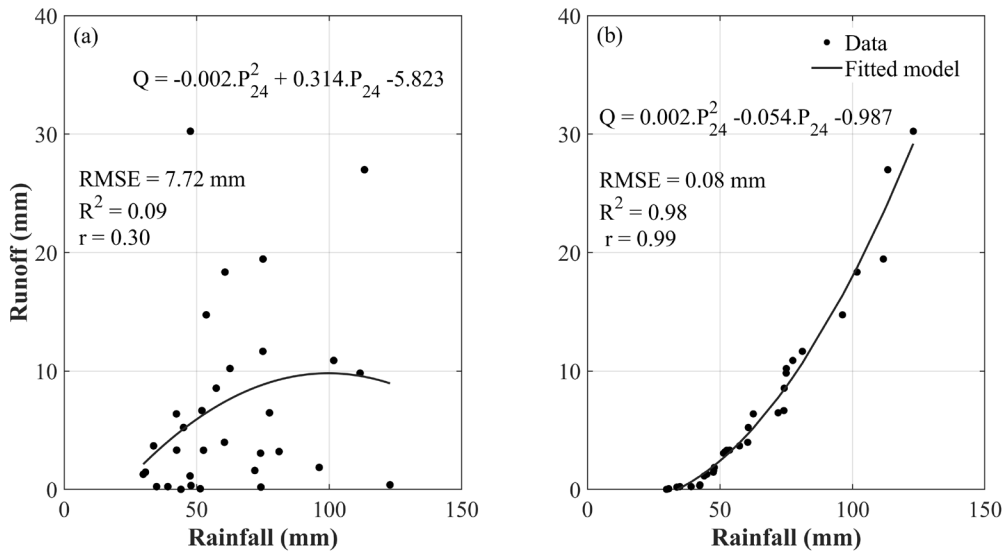
Figure 5. The relationship between measured 24-hour rainfall (P_{24}) data and calculated runoff (Q) for the ICP clogging condition: (a) Natural-ordered data; and (b) Rank-ordered data. Runoff was computed using the HORTORUN method. *RMSE* is the Root Mean Squared Error, R^2 is the coefficient of determination, and r is the Pearson's coefficient of correlation.
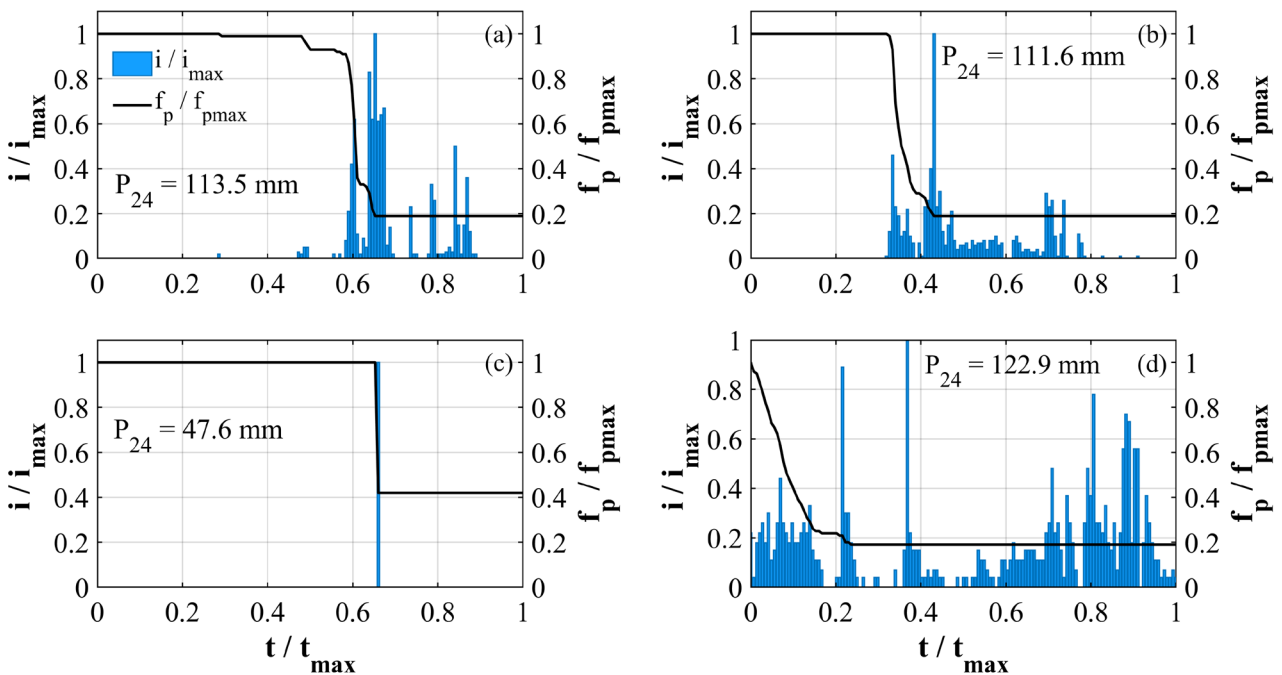
Figure 6. Normalized hyetographs of rainfall intensity (i / i_{max}) and normalized infiltration capacity (f_p / f_{pmax}) curves over normalized time (t / t_{max}) for different 24-hour rainfall depths (P_{24}): (a) $P_{24} = 113.5$ mm; (b) $P_{24} = 111.6$ mm; (c) $P_{24} = 47.6$ mm; and (d) $P_{24} = 122.9$ mm. The i_{max}, f_{pmax}, and t_{max} are the maximum rainfall intensity, infiltration capacity and time of each event. All rainfall events have 24-hour duration.

of America territory. Our results also agree with the other study (Wang & Bi, 2020) that used a rainfall simulator at a plot scale to demonstrate the effect of rainfall intensity and duration on Q, S, CN, and λ.

Curve Number and initial abstraction estimates

Overall, we observed that CN values under clogged condition ranged slightly from 64.7 to 56.4 (with $\overline{\text{CN}}$ = 61.7 and $\widetilde{\text{CN}}$ = 62.2) for λ = 0.20 and from 48.5 to 30.8 (with $\overline{\text{CN}}$ = 40.2 and $\widetilde{\text{CN}}$ = 41.1) for λ = 0.05, considering the 32 P_{24}-Q events (Table 1). We found the CN = 52.2 (natural-ordered data) and the CN = 60.1 (rank-ordered data), both for λ = 0.20, using the Least-squares method (Table 1). Further, for λ = 0.20 we found the CN = 36.5 (natural-ordered data) and the CN = 44.4 (rank-ordered data) using the Least-squares method. Bean et al. (2007) reported CN values ranging from 37 to 50 (with $\overline{\text{CN}}$ = 44 and $\widetilde{\text{CN}}$ = 45) for PICP at plot scale. Thus, our results are consistent because CN values for the clogged ICP were higher than those for PICP.

Although results demonstrate that the P_{24} did not explain the Q for natural ordered data (Figure 5a), we assessed the relationship between CN and P_{24} for rank-ordered data using Asymptotic fit method (Hawkins, 1993).

Results showed a standard behavior for λ = 0.20 (Figure 7a) and violent behavior for λ = 0.05 (Figure 7a) using the asymptotic fit method. Hence, we found that CN behavior is strongly affected by the initial abstraction ratio for the clogged ICP material. The standard and violent behavior revealed a CN_∞ = 60.7 and CN_∞ = 42.3, respectively (Table 1). However, the goodness of fit was unsatisfactory for both standard (R^2 = 0.26) and violent behavior (R^2 = 0.30).

We compared the CN results of CN (Table 1) using the P_{24}-Q relation using the CN method formulation. We found that the CN estimates fitted better to the P_{24}-Q relation for λ = 0.20 (Figure 8a, c) than for λ = 0.05 (Figure 8b, c) regardless the CN estimating method (Least-squares, Median, Mean, or Asymptotic). Further, it is clear that the simulated runoff values were overestimated using λ = 0.05 (Figure 8b, d). Hence, the usage of λ = 0.05 was inappropriate to estimate runoff depth under the clogged ICP material.

We also observed that the CN estimating methods did not differ significantly to fit the P_{24}-Q relation (Figure 8). Nevertheless, the least-squares method presented performance (R^2 = 0.97 and $RMSE$ = 1.45 mm) using rank-ordered data to simulate runoff depth. Thus, in practice, the most suitable CN values for natural- and rank-ordered data (λ = 0.20) are equal to 52.2 and 60.1, respectively, considering the intrarainfall application of the CN method.

Table 1. The summary of Curve Number estimates for two initial abstraction ratios (λ = 0.20 and λ = 0.05) using natural and rank-ordered data. The CN is valid for the clogged ICP. The "–" indicates no CN value, and "*" means the asymptotic CN (CN_∞).

Method	Curve Number (CN)			
	Natural-ordered data (λ = 0.20)	Rank-ordered data (λ = 0.20)	Natural-ordered data (λ = 0.05)	Rank-ordered data (λ = 0.05)
Mean	61.7	61.7	40.2	40.2
Median	62.7	62.7	41.1	41.1
Least-squares	52.2	60.1	36.5	44.4
Asymptotic fit	–	60.7*	–	42.3*
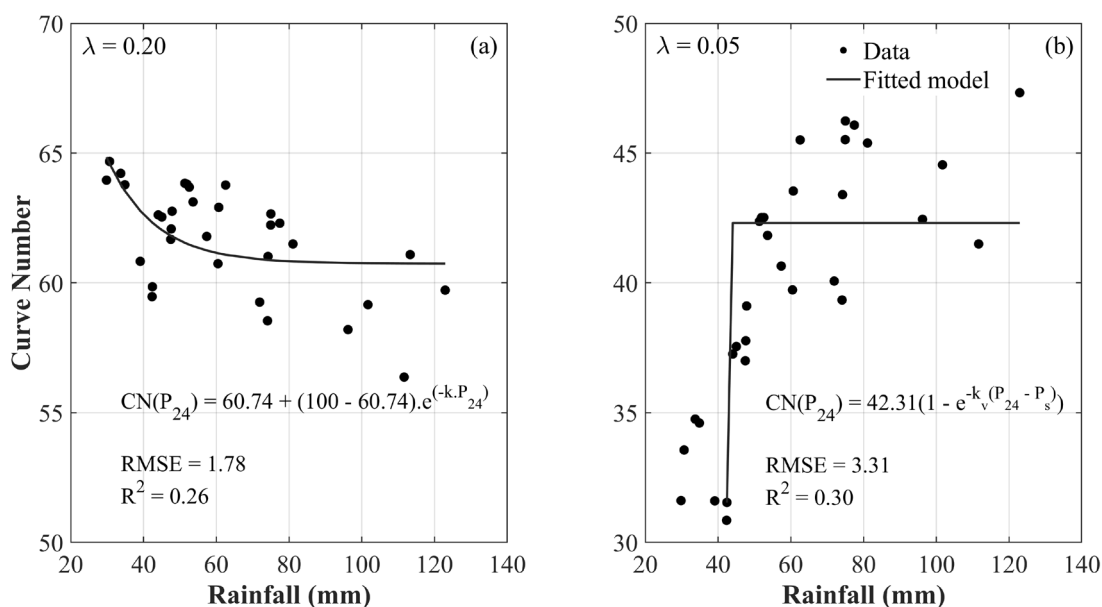
Figure 7. Asymptotic fit method using rank-ordered rainfall (P_{24}) and runoff (Q) data for: (a) λ = 0.20 (standard behavior); and (b) λ = 0.05 (violent behavior). The threshold rainfall depth (P_s) is equal to 42.34 mm in violent behavior. The Curve Numbers are valid for the clogged ICP surface, $RMSE$ is the Root Mean Squared Error, and R^2 is the coefficient of determination.
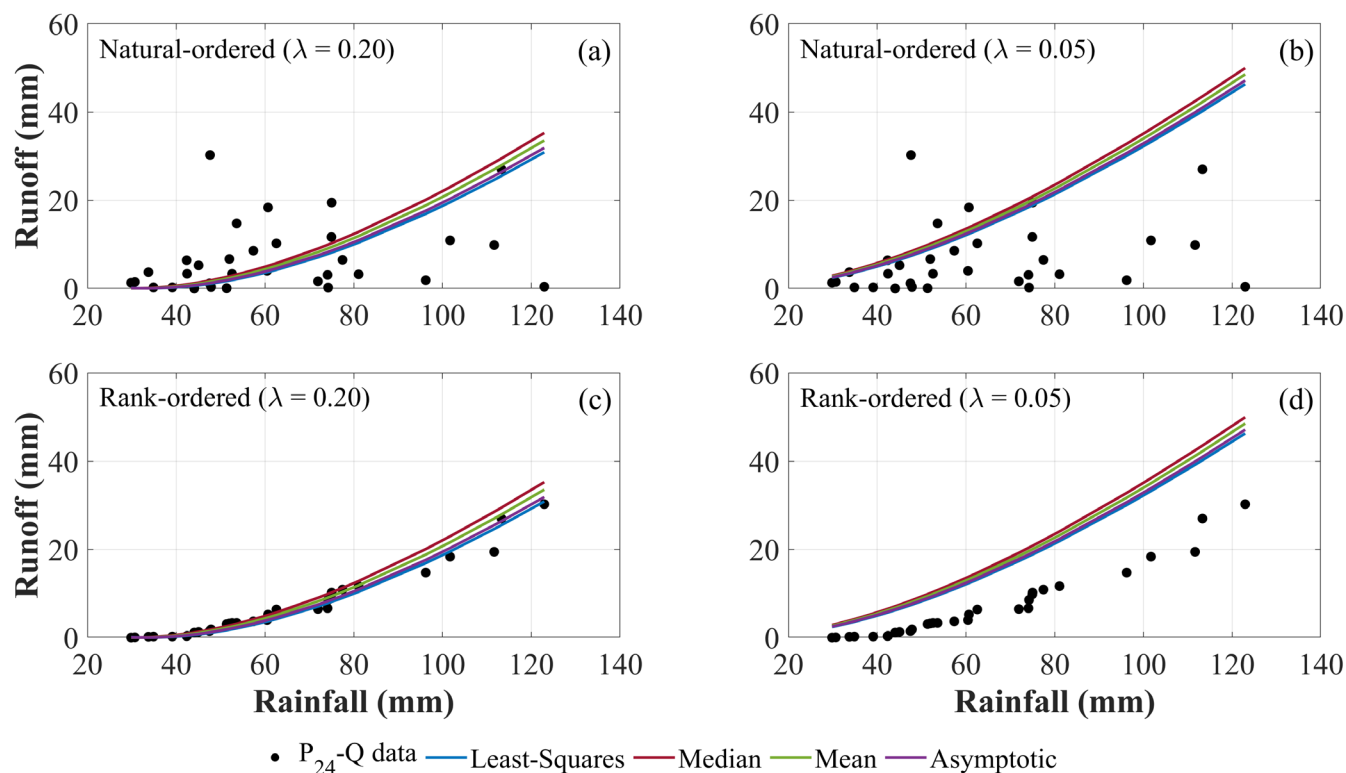
Figure 8. The CN estimating methods (Least-squares, Median, Mean, and Asymptotic fit) for the relationship between rainfall (P_{24}) and runoff (Q): (a) Natural-ordered data ($\lambda = 0.20$); (b) Natural-ordered data ($\lambda = 0.05$); (c) Rank-ordered data ($\lambda = 0.20$); and (d) Rank-ordered data ($\lambda = 0.05$).

CONCLUSION

We present the initial abstraction ratio (λ) and Curve Number (CN) values for runoff estimating in interlocking concrete pavement (ICP) material. It is essential to mention that the ICP is seated over bare soil (not over a permeable pavement structure), and CN estimates are valid for the clogged ICP condition because the unclogged ICP did not generate runoff. Further, our CN values do not account for runoff from surrounding areas, that is, runoff generation occurs only from rainfall that falls directly over the ICP material. We concluded that the temporal distribution and intensity of 24-hour rainfall depth are essential characteristics to explain runoff generation under the incremental approach. We noted that $\lambda = 0.20$ is appropriate to estimate runoff for ICP material instead of the ongoing value of $\lambda = 0.05$. Finally, we demonstrated that representative CN values are equal to 52.2 (natural-ordered data) and 60.1 (rank-ordered data), respectively. Therefore, our findings can improve the accuracy of rainfall-runoff simulations and, consequently, stormwater drainage system design to mitigate urban flooding.

DATA AVAILABILITY STATEMENTS

All data, models, or code that support the findings of this study are available from the corresponding author upon reasonable request.

REFERENCES

Ajmal, M., Waseem, M., Ahn, J.-H., & Kim, T.-W. (2016). Runoff estimation using the NRCS slope-adjusted curve number in mountainous watersheds. *Journal of Irrigation and Drainage Engineering*, *142*(4), 04016002. http://dx.doi.org/10.1061/(ASCE)IR.1943-4774.0000998.

Alvares, C. A., Stape, J. L., Sentelhas, P. C., de Moraes Gonçalves, J. L., & Sparovek, G. (2013). Köppen's climate classification map for Brazil. *Meteorologische Zeitschrift (Berlin)*, *22*(6), 711-728. http://dx.doi.org/10.1127/0941-2948/2013/0507.

American Society for Testing and Materials – ASTM. (2013). *C1781: Standard test method for surface infiltration rate of permeable unit pavement systems*. West Conshohocken: ASTM International.

Assaye, H., Nyssen, J., Poesen, J., Lemma, H., Meshesha, D. T., Wassie, A., Adgo, E., & Frankl, A. (2021). Curve number calibration for measuring impacts of land management in sub-humid Ethiopia. *Journal of Hydrology: Regional Studies*, *35*, 100819. http://dx.doi.org/10.1016/J.EJRH.2021.100819.

Bazzo, J. A., & Horn, P. L. (2017). *Calibração do modelo matemático de infiltração de Horton em pavimento de concreto tipo blocos intertravados* (Trabalho de Conclusão de Curso). Universidade Tecnológica

Federal do Paraná, Pato Branco. Retrieved in 2022, May 15, from http://repositorio.utfpr.edu.br/jspui/handle/1/14558

Bean, E. Z., Hunt, W. F., & Bidelspach, D. A. (2007). Field survey of permeable pavement surface infiltration rates. *Journal of Irrigation and Drainage Engineering*, *133*(3), 249-255. http://dx.doi.org/10.1061/(ASCE)0733-9437(2007)133:3(249).

Beecham, S., Pezzaniti, D., & Kandasamy, J. (2012). Stormwater treatment using permeable pavements. *Proceedings of the Institution of Civil Engineers: Water Management*, *165*(3), 161-170. https://doi.org/10.1680/wama.2012.165.3.161.

Bertotto, L. E., Lucas, M. C., Destro, C. A. M., Chin, D. A., Alves, W. S., & de Oliveira, P. T. S. (2021). Effects of infiltration conditions and rainfall characteristics on simulated curve numbers. *Journal of Irrigation and Drainage Engineering*, *147*(10), 05021004. http://dx.doi.org/10.1061/(ASCE)IR.1943-4774.0001605.

Brasil. Ministério da Ciência, Tecnologia, Inovações e Comunicações. Centro Nacional de Monitoramento e Alertas de Desastres Naturais. (2022). *Mapa Interativo da Rede Observacional para Monitoramento de Risco de Desastres Naturais do Cemaden*. Retrieved in 2022, May 15, from http://www2.cemaden.gov.br/mapainterativo

Cao, H., Willem Vervoort, R., & Dabney, S. M. (2011). Variation in curve numbers derived from plot runoff data for New South Wales (Australia). *Hydrological Processes*, *25*(24), 3774-3789. https://doi.org/10.1002/hyp.8102.

Chin, D. A. (2013). *Water-resources engineering* (3rd ed). London: Pearson Education.

Chin, D. A. (2017). Estimating the parameters of the curve number model. *Journal of Hydrologic Engineering*, *22*(6), 06017001. http://dx.doi.org/10.1061/(ASCE)HE.1943-5584.0001495.

Chin, D. A. (2021). Deficiencies in the curve number method. *Journal of Irrigation and Drainage Engineering*, *147*(5), 04021008. http://dx.doi.org/10.1061/(ASCE)IR.1943-4774.0001552.

Collins, K. A., Hunt, W. F., & Hathaway, J. M. (2008). Hydrologic comparison of four types of permeable pavement and standard asphalt in Eastern North Carolina. *Journal of Hydrologic Engineering*, *13*(12), 1146-1157. http://dx.doi.org/10.1061/(ASCE)1084-0699(2008)13:12(1146).

D'Asaro, F., Grillone, G., & Hawkins, R. H. (2014). Curve number: empirical evaluation and comparison with curve number handbook tables in sicily. *Journal of Hydrologic Engineering*, *19*(12), 04014035. http://dx.doi.org/10.1061/(ASCE)HE.1943-5584.0000997.

Damodaram, C., Giacomoni, M. H., Prakash Khedun, C., Holmes, H., Ryan, A., Saour, W., & Zechman, E. M. (2010). Simulation of combined best management practices and low impact development for sustainable stormwater management1. *Journal of the American Water Resources Association*, *46*(5), 907-918. http://dx.doi.org/10.1111/J.1752-1688.2010.00462.X.

Dingman, L. S. (2015). *Physical hydrology* (3rd ed). Illinois: Waveland Press, Inc.

Durán-Barroso, P., González, J., & Valdés, J. B. (2017). Sources of uncertainty in the NRCS CN model: recognition and solutions. *Hydrological Processes*, *31*(22), 3898-3906. http://dx.doi.org/10.1002/HYP.11305.

Galbetti, M. V., Zuffo, A. C., Shinma, T. A., Boulomytis, V. T. G., & Imteaz, M. (2021). Evaluation of the tabulated, NEH4, least squares and asymptotic fitting methods for the CN estimation of urban watersheds. *Urban Water Journal*, *19*(3), 244-255. https://doi.org/10.1080/1573062X.2021.1992639.

Grimaldi, S., Petroselli, A., & Romano, N. (2013). Green-Ampt Curve-Number mixed procedure as an empirical tool for rainfall–runoff modelling in small and ungauged basins. *Hydrological Processes*, *27*(8), 1253-1264. http://dx.doi.org/10.1002/HYP.9303.

Hawkins, R. H. (1993). Asymptotic determination of runoff curve numbers from data. *Journal of Irrigation and Drainage Engineering*, *119*(2), 334-345. http://dx.doi.org/10.1061/(ASCE)0733-9437(1993)119:2(334).

Hawkins, R. H. (2014). Curve number method: time to think anew? *Journal of Hydrologic Engineering*, *19*(6), 1059. http://dx.doi.org/10.1061/(ASCE)HE.1943-5584.0000954.

Horton, R. E. (1933). The Rôle of infiltration in the hydrologic cycle. *Eos (Washington, D.C.)*, *14*(1), 446-460. http://dx.doi.org/10.1029/TR014I001P00446.

Hu, P., Tang, J., Fan, J., Shu, S., Hu, Z., & Zhu, B. (2020). Incorporating a rainfall intensity modification factor γ into the Ia-S Relationship in the NRCS-CN method. *International Soil and Water Conservation Research*, *8*(3), 237-244. http://dx.doi.org/10.1016/J.ISWCR.2020.07.004.

Im, S., Lee, J., Kuraji, K., Lai, Y. J., Tuankrua, V., Tanaka, N., Gomyo, M., Inoue, H., & Tseng, C. W. (2020). Soil conservation service curve number determination for forest cover using rainfall and runoff data in experimental forests. *Journal of Forest Research*, *25*(4), 204-213. https://doi.org/10.1080/13416979.2020.1785072.

Jain, M. K., Mishra, S. K., Babu, P. S., Venugopal, K., & Singh, V. P. (2006). Enhanced runoff curve number model incorporating storm duration and a nonlinear Ia-S Relation. *Journal of Hydrologic Engineering*, *11*(6), 631-635. http://dx.doi.org/10.1061/(ASCE)1084-0699(2006)11:6(631).

Karpathy, N. S., & Chin, D. A. (2019). Relationship between Curve Number and φ-Index. *Journal of Irrigation and Drainage Engineering*, *145*(11), 06019009. http://dx.doi.org/10.1061/(asce)ir.1943-4774.0001426.

Lal, M., Mishra, S. K., Pandey, A., Pandey, R. P., Meena, P. K., Chaudhary, A., Jha, R. K., Shreevastava, A. K., & Kumar, Y. (2017). Evaluation de la méthode du numéro de courbe du Service de la

Conservation des Sols à partir de données provenant de parcelles agricoles. *Hydrogeology Journal*, *25*(1), 151-167. http://dx.doi.org/10.1007/S10040-016-1460-5/FIGURES/9.

Legret, M., Nicollet, M., Miloda, P., Colandini, V., & Raimbault, G. (1999). Simulation of heavy metal pollution from stormwater infiltration through a porous pavement with reservoir structure. *Water Science and Technology*, *39*(2), 119-125. http://dx.doi.org/10.1016/S0273-1223(99)00015-3.

Levenberg, K. (1944). A method for the solution of certain non-linear problems in least squares. *Quarterly of Applied Mathematics*, *2*(2), 164-168. Retrieved in 2022, May 15, from http://www.jstor.org/stable/43633451

Liu, W., Chen, W., & Feng, Q. (2018). Field simulation of urban surfaces runoff and estimation of runoff with experimental curve numbers. *Urban Water Journal*, *15*(5), 418-426. https://dx.doi.org/10.1080/1573062X.2018.1508597.

Liu, Y., Li, T., & Yu, L. (2020). Urban heat island mitigation and hydrology performance of innovative permeable pavement: a pilot-scale study. *Journal of Cleaner Production*, *244*, 118938. http://dx.doi.org/10.1016/J.JCLEPRO.2019.118938.

Lucke, T., White, R., Nichols, P., & Borgwardt, S. (2015). A simple field test to evaluate the maintenance requirements of permeable interlocking concrete pavements. *Water*, *7*(6), 2542-2554. https://dx.doi.org/10.3390/W7062542.

Marquardt, D. W. (1963). An algorithm for least-squares estimation of nonlinear parameters. *Journal of the Society for Industrial and Applied Mathematics*, *11*(2), 431-441. Retrieved in 2022, May 15, from http://www.jstor.org/stable/2098941

Martin, W. D., & Kaye, N. B. (2014). Hydrologic characterization of undrained porous pavements. *Journal of Hydrologic Engineering*, *19*(6), 1069-1079. https://doi.org/10.1061/(ASCE)HE.1943-5584.0000873.

Michel, C., Andréassian, V., & Perrin, C. (2005). Soil Conservation Service Curve Number method: how to mend a wrong soil moisture accounting procedure? *Water Resources Research*, *41*(2), 1-6. http://dx.doi.org/10.1029/2004WR003191.

Moglen, G. E., Sadeq, H., Hughes, L. H., Meadows, M. E., Miller, J. J., Ramirez-Avila, J. J., & Tollner, E. W. (2022). NRCS curve number method: comparison of methods for estimating the curve number from Rainfall-Runoff Data. *Journal of Hydrologic Engineering*, *27*(10), 4022023. http://dx.doi.org/10.1061/(ASCE)HE.1943-5584.0002210.

Oliveira, P. T. S., Nearing, M. A., Hawkins, R. H., Stone, J. J., Rodrigues, D. B. B., Panachuki, E., & Wendland, E. (2016). Curve number estimation from Brazilian Cerrado rainfall and runoff data. *Journal of Soil and Water Conservation*, *71*(5), 420-429. http://dx.doi.org/10.2489/JSWC.71.5.420.

Palla, A., & Gnecco, I. (2015). Hydrologic modeling of Low Impact Development systems at the urban catchment scale. *Journal of Hydrology (Amsterdam)*, *528*, 361-368. http://dx.doi.org/10.1016/J.JHYDROL.2015.06.050.

Ponce, V. M., & Hawkins, R. H. (1996). Runoff curve number: has it reached maturity? *Journal of Hydrologic Engineering*, *1*(1), 11-19. http://dx.doi.org/10.1061/(ASCE)1084-0699(1996)1:1(11).

Pratt, C. J., Newman, A. P., & Bond, P. C. (1999). Mineral oil bio-degradation within a permeable pavement: long term observations. *Water Science and Technology*, *39*(2), 103-109. http://dx.doi.org/10.1016/S0273-1223(99)00013-X.

Sahu, R. K., Mishra, S. K., & Eldho, T. I. (2012). Improved storm duration and antecedent moisture condition coupled SCS-CN Concept-Based Model. *Journal of Hydrologic Engineering*, *17*(11), 1173-1179. http://dx.doi.org/10.1061/(ASCE)HE.1943-5584.0000443.

Schwartz, S. S. (2010). Effective curve number and hydrologic design of pervious concrete storm-water systems. *Journal of Hydrologic Engineering*, *15*(6), 465-474. http://dx.doi.org/10.1061/(ASCE)HE.1943-5584.0000140.

Shi, W., Wang, N., Wang, M., & Li, D. (2021). Revised runoff curve number for runoff prediction in the Loess Plateau of China. *Hydrological Processes*, *35*(10), e14390. http://dx.doi.org/10.1002/HYP.14390.

Tabalipa, N. L. (2008). *Estudo da estabilidade de vertentes da bacia do rio Ligeiro, Pato Branco, Paraná* [Tese de doutorado). Universidade Federal do Paraná, Curitiba. Retrieved in 2022, May 15, from https://acervodigital.ufpr.br/handle/1884/21252

United States Department of Agriculture – USDA. (1986). Urban Hydrology for Small Watersheds.

United States Department of Agriculture – USDA. (2004). Hydrologic Soil- Cover Complexes. In United States Department of Agriculture – USDA. *National Engineering Handbook: Part 630 Hydrology* (pp. 20). USA: United States Department of Agriculture (USDA) and Natural Resources Conservation Service (NRCS).

United States Department of Agriculture – USDA. (2017). Estimation of direct runoff from storm rainfall (draft). In United States Department of Agriculture – USDA. *National Engineering Handbook: Part 630 Hydrology* (pp. 45). USA: United States Department of Agriculture (USDA) and Natural Resources Conservation Service (NRCS).

Valle Junior, L. C. G., Rodrigues, D. B. B., & de Oliveira, P. T. S. (2019). Initial abstraction ratio and Curve Number estimation using rainfall and runoff data from a tropical watershed. *Revista Brasileira de Recursos Hídricos*, *24*, http://dx.doi.org/10.1590/2318-0331.241920170199.

Verma, S., Singh, P. K., Mishra, S. K., Singh, V. P., Singh, V., & Singh, A. (2020). Activation soil moisture accounting (ASMA) for runoff estimation using soil conservation service curve number

(SCS-CN) method. *Journal of Hydrology (Amsterdam)*, *589*, 125114. http://dx.doi.org/10.1016/J.JHYDROL.2020.125114.

Wang, X., & Bi, H. (2020). The effects of rainfall intensities and duration on SCS-CN model parameters under simulated rainfall. *Water, 12*(6), 1595. https://doi.org/10.3390/W12061595.

Winston, R. J., Arend, K., Dorsey, J. D., Johnson, J. P., & Hunt, W. F. (2019). Hydrologic performance of a permeable pavement and stormwater harvesting treatment train stormwater control measure. *Journal of Sustainable Water in the Built Environment*, *6*(1), 04019011. http://dx.doi.org/10.1061/JSWBAY.0000889.

Woods-Ballard, B., Wilson, S., Udale-Clarke, H., Illman, S., Scott, T., Ashley, R., & Kellagher, R. (2015). *The SuDS Manual.* London: CIRIA.

Woodward, D. E., Hawkins, R. H., Jiang, R., Hjelmfelt Junior, A. T., Van Mullem, J. A., & Quan, Q. D. (2003). Runoff curve number method: examination of the initial abstraction ratio. *World Water & Environmental Resources Congress*, *2003*, 1-10. http://dx.doi.org/10.1061/40685(2003)308.

Authors contributions

Murilo Cesar Lucas: Conceptualization, Supervision, Project administration, Investigation, Formal analysis, Writing – original draft.

Gustavo Bonfim Jodas: Data curation, Investigation, Formal analysis, Methodology, Writing – review & editing.

Luis Eduardo Bertotto: Data curation, Investigation, Formal analysis, Methodology, Writing – review & editing.

Paulo Tarso Sanches de Oliveira: Formal analysis, Methodology, Writing – review & editing

Alessandro Bail: Formal analysis, Methodology, Writing – review & editing.

Editor in-Chief: Adilson Pinheiro

Associated Editor: Priscilla Macedo Moura

SUPPLEMENTARY MATERIAL

Supplementary material accompanies this paper.

Table S1. Summary of the 24-hour rainfall events.